Supporting Information

Small Energy Loss in Ternary Organic Solar Cells with a Blend of Cascade Energy Levels Two Fullerene-Free Acceptors as the Electron Acceptor

Zhiyong Liu[a*], Ning Wang[b*]

[a]College of Science, Shenyang Agricultural University, Shenyang 110866, People's Republic of China

[b]Key Laboratory of Physics and Technology for Advanced Batteries (Ministry of Education), College of Physics, Jilin University, Changchun 130012, China

[*]Corresponding authors: (zhyliu2006@syau.edu.cn (Z.Y. Liu); eningwang@outlook.com (N. Wang))

2. Experimental details

2.1 Materials

4TIC and IEICO-4F were purchased from 1-Material Inc. PBDB-T was purchased from Luminescence Technology Co. *o*-dichlor-obenzene (ODCB) and 1,8-diiodooctane (DIO) were purchased from Sigma-Aldrich Co. MoO_3 and Ag were purchased from Alfa Aesar Co. The blend of PBDB-T, IEICO-4F and 4TIC (the concentration is 25 mg mL^{-1} in total) was dissolved in ODCB as a function of the ratio of IEICO-4F:4TIC and stirred overnight. The ZnO solution was synthesized by the sol-gel method [1, 2].

2.2 OSCs device preparation and characteristics

Indium–tin-oxide (ITO) glasses were ultrasonicated at 30 °C in isopropyl alcohol, acetone and deionized water for 30 min, respectively. The ITO glasses were then dried by a stream of nitrogen and heated on the hot-stage. The ZnO solution was spin-coated onto the ITO glass and baked at 150 °C for 20 min in air (the thickness of ZnO thin films is 20 nm). The blended solution was spin-coated on the ZnO layer in a N_2-filled glove box to form the photoactive layer, and the thermal annealing treatment was carried out (the nominal thickness of ~90 nm). A MoO_3 layer and a Ag electrode were evaporated under vacuum through a shadow mask to define the active area of the devices (3×3 mm^2). The current density versus voltage (*J*–*V*) characteristics of OSCs were measured in a glove box with a computer-controlled Keithley 236 Source Measure Unit under illumination at 100 mW cm^{-2} using an AM1.5 G solar simulator. The external quantum efficiency (*EQE*) spectrum was measured with a Stanford Research

Systems model SR830 DSP lock-in amplifier coupled to a WDG3 monochromator and a 500 W xenon lamp.

2.3 SCLC device preparation and characteristics

The hole-only space-charge-limited-current (SCLC) devices and electron-only SCLC devices were fabricated with the structures of ITO/PEDOT:PSS/PBDB-T:IEICO-4F:4TIC/Au and Al/PBDB-T:IEICO-4F:4TIC/Al, respectively. The charge carrier mobilities were calculated using the equation [3, 4]:

$$J = \frac{9}{8}\varepsilon_r\varepsilon_0\mu\frac{V^2}{d^3}$$

where J is the current density, μ is the charge carrier mobility, ε_0 (8.85×10^{-14} F/cm) and ε_r are the permittivity of free space and relative permittivity of the material (ε_r was assumed to be 3), respectively, and V is the SCLC effective voltage. The charge carrier mobility were calculated using the equation [5]:

$$\mu = \mu_0 \exp[0.89\gamma\sqrt{\frac{V}{L}}]$$

where μ_0 is the charge mobility under zero electric field and γ is a constant. Then, the Mott-Gurney equation can be described by [6]:

$$J = \frac{9}{8}\varepsilon_r\varepsilon_0\mu_0\frac{V^2}{L^3}\exp[0.89\gamma\sqrt{\frac{V}{L}}]$$

In this case, the charge mobility were estimated using the following equation [6]:

$$\ln(\frac{JL^3}{V^2}) = 0.89\gamma\sqrt{\frac{V}{L}} + \ln(\frac{9}{8}\varepsilon_r\varepsilon_0\mu_0)$$

2.4 XRD calculated and characteristics

The angles at which the peak intensities occur are related to the inter-planar distances of the atomic structure of the photoactive layer and the crystallinity of

photoactive layer; these angles are related by Bragg's law [7]:

$$\lambda = 2d\sin\theta$$

where λ is the wavelength of the X-ray radiation used (0.154 nm), θ is the peak position half-angle, and *d* is the inter-planar distance.

2.5 Surface energy calculated and characteristics

The surface energy of pristine PBDB-T, IEICO-4F and 4TIC were achieved the other paper and summarized at Table S3 [8-10]. The interfacial surface energy between different materials in the blend can be calculated using the followed equation:

$$\gamma_{1-2} = \gamma_1 + \gamma_2 - 2\sqrt{\gamma_1 \times \gamma_2}e^{\left[-\beta(\gamma_1-\gamma_2)^2\right]}$$

Where $\gamma_{1\text{-}2}$ is the interfacial surface energy between materials 1 and materials 2 and β is 0.000115 m^4/mJ^2. The calculated γ value of PBDB-T:IEICO-4F, IEICO-4F:4TIC and PBDB-T:4TIC binary films are summarized at Table S4. The wetting coefficient (ω) of the third component in the binary photoactive layer can be calculated and according to the Young's formula:

$$\omega = \frac{\gamma_{\text{Third-IEICO-4F}} - \gamma_{\text{Third-PBDB-T}}}{\gamma_{\text{Binary}}}$$

The 4TIC were defined as third component materials.

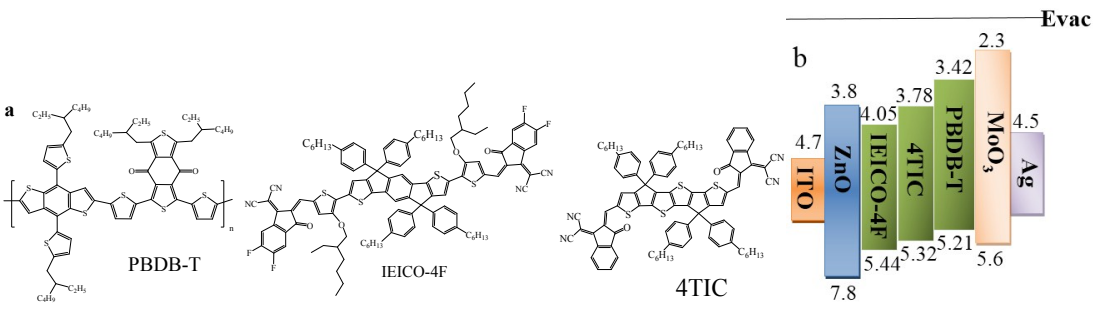

Figure S1. (a) Chemical structures of PBDB-T, IEICO-4F and 4TIC. (b) The energy

level of OSCs.

Table S1. Summary of molecular weight, *n*, *l*, and N_e values of IEICO-4F and 4TIC.

Electron Acceptor	Molecular Weight (g mol^{-1})	*n* (mol g^{-1})	*l*	N_e (mol g^{-1})
IEICO-4F	2054	2.93×10^{20}	1	2.93×10^{-3}
4TIC	1895	3.18×10^{20}	1	3.18×10^{-3}

Table S2. Summary of V_{OC}, E_g and E_{loss} values of all the OSCs depending on the ratio of IEICO-4F:4TIC.

IEICO-4F :4TIC	V_{OC} (V)	E_g (eV)	E_{loss} (eV)
100:0	0.72	1.16	0.44
50:50	0.80	1.22	0.42
55:45	0.81	1.22	0.41
60:40	0.82	1.23	0.41
65:35	0.81	1.23	0.42
70:30	0.83	1.27	0.44
0:100	0.84	1.43	0.59

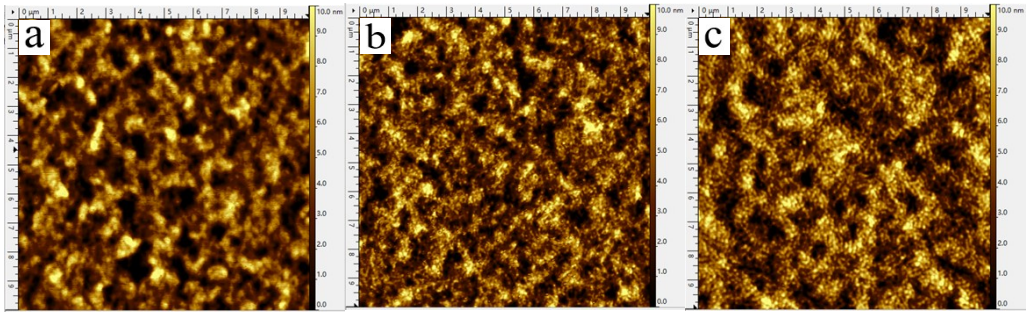

Figure S2 AFM images of PBDB-T:IEICO-4F:4TIC with ratios of IEICO-4F:4TIC of 100:0 (a), 60:40 (b), and 0:100 (c).

Table S3 Surface energy of PBDB-T, IEICO-4F and 4TIC.

	PBDB-T	IEICO-4F	4TIC

Surface energy (mJ cm^{-2})	25.25	27.75	32.24

Table S4 Interfacial surface energy between components 1 and 2 in different blends.

	PBDB-T :IEICO-4F	IEICO-4F: 4TIC	PBDB-T :4TIC
Wettin g	0.3588	0.1857	0.7463

Table S5 Wetting coefficient of ternary photoactive layer.

	Ternary Film
ω	-1.56

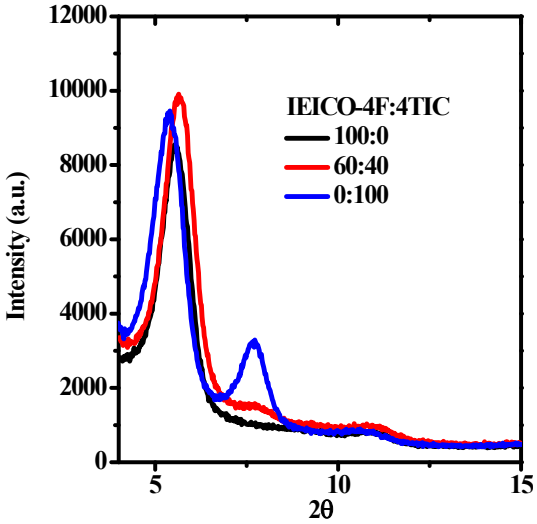

Figure S3. XRD curves of PBDB-T:IEICO-4F binary thin films, PBDB-T:IEICO-4F:4TIC ternary thin films and PBDB-T:4TIC binary thin films.

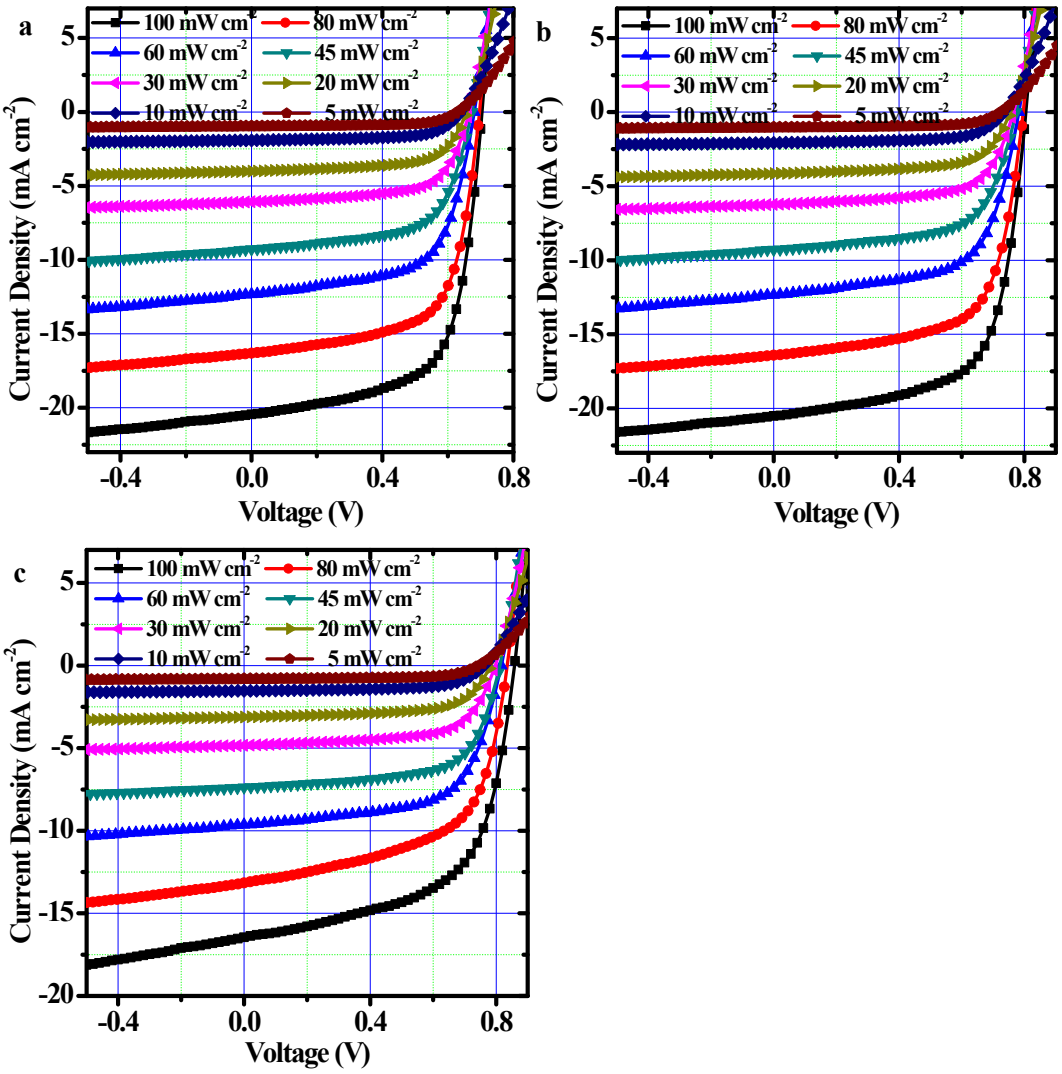

Figure S4. *J-V* characteristics of the OSCs under various light intensities ranging from 100 mW cm^{-2} to 5 mW cm^{-2} with ratios of IEICO-4F:4TIC of 100:0, 60:40 and 0:100 corresponding to Figure S4(a), S4(b) and S4(c), respectively.

Reference:

[1] W. Yu, L. Huang, D. Yang, P. Fu, L. Zhou, J. Zhang, C. Li, Efficiency exceeding 10% for inverted polymer solar cells with a ZnO/ionic liquid combined cathode interfacial layer, Journal of Materials Chemistry A, 3 (2015) 10660-10665.

[2] U. Galan, Y. Lin, G.J. Ehlert, H.A. Sodano, Effect of ZnO nanowire morphology on the interfacial strength of nanowire coated carbon fibers, Composites Science and Technology, 71 (2011) 946-954.

[3] H.-W. Li, Z. Guan, Y. Cheng, T. Lui, Q. Yang, C.-S. Lee, S. Chen, S.-W. Tsang, On the Study of Exciton Binding Energy with Direct Charge Generation in Photovoltaic Polymers, Advanced Electronic Materials, 2 (2016) 1600200-1600209.

[4] V. Narasimhan, D. Jiang, S.-Y. Park, Design and optical analyses of an arrayed microfluidic tunable prism panel for enhancing solar energy collection, Applied Energy, 162 (2016) 450-459.

[5] Q. An, F. Zhang, Q. Sun, M. Zhang, J. Zhang, W. Tang, X. Yin, Z. Deng, Efficient organic ternary solar cells with the third component as energy acceptor, Nano Energy, 26 (2016) 180-191.

[6] Q. An, F. Zhang, W. Gao, Q. Sun, M. Zhang, C. Yang, J. Zhang, High-efficiency and air stable fullerene-free ternary organic solar cells, Nano Energy, 45 (2018) 177-183.

[7] L. Zhao, S. Zhao, Z. Xu, Q. Yang, D. Huang, X. Xu, A simple method to adjust the morphology of gradient three-dimensional PTB7-Th:PC71BM polymer solar cells, Nanoscale, 7 (2015) 5537-5544.

[8] X. Liu, B. Xie, C. Duan, Z. Wang, B. Fan, K. Zhang, B. Lin, F.J.M. Colberts, W. Ma, R.A.J. Janssen, F. Huang, Y. Cao, A high dielectric constant non-fullerene acceptor for efficient bulk-heterojunction organic solar cells, Journal of Materials Chemistry A, 6 (2018) 395-403.

[9] X. Shi, J. Chen, K. Gao, L. Zuo, Z. Yao, F. Liu, J. Tang, A.K.Y. Jen, Terthieno[3,2-b]Thiophene (6T) Based Low Bandgap Fused-Ring Electron Acceptor for Highly Efficient Solar Cells with a High Short-Circuit Current Density and Low Open-Circuit Voltage Loss, Advanced Energy Materials, 8 (2018) 1702831-1702838.

[10] X. Shi, L. Zuo, S.B. Jo, K. Gao, F. Lin, F. Liu, A.K.Y. Jen, Design of a Highly Crystalline Low-Band Gap Fused-Ring Electron Acceptor for High-Efficiency Solar Cells with Low Energy Loss, Chemistry of Materials, 29 (2017) 8369-8376.